Renewable Energy 146 (2020) 444–459

Contents lists available at ScienceDirect

Renewable Energy

journal homepage: www.elsevier.com/locate/renene

The performance of the three-float M4 wave energy converter off Albany, on the south coast of western Australia, compared to Orkney (EMEC) in the U.K.

H. Santo [a, *], P.H. Taylor [b], P.K. Stansby [c]

[a] Technology Centre for Offshore and Marine, Singapore (TCOMS), Singapore, 118411, Singapore
[b] Faculty of Engineering and Mathematical Sciences, University of Western Australia, Crawley, WA 6009, Australia
[c] School of Mechanical, Aerospace and Civil Engineering, University of Manchester, Manchester, M13 9PL, UK

ARTICLE INFO

Article history:
Received 13 December 2018
Received in revised form
16 April 2019
Accepted 25 June 2019
Available online 28 June 2019

Keywords:
M4 wave energy converter
Extreme wave height
Practical wave power
Extreme response
South coast of western Australia
Orkney (EMEC)

ABSTRACT

In this study we compare wave climates and their potential for wave energy conversion for the two energetic but quite different sites of Albany and Orkney. Energy capture is based on the M4 machine with well defined characteristics. The M4 machine is a self reacting system with 3 floats, each float with a circular cross-section when viewed from above. The smaller two floats are rigidly connected by a beam, and the largest float is connected to the mid float by a beam with a hinge. The machine generates power through the relative angular motion of this hinge above the middle float. The machine performance was previously assessed for various locations in the eastern North Atlantic including the European Marine Energy Centre (EMEC) site west of the Orkney Islands, Scotland, for wave power output (Santo et al., 2016a) and extreme response (Santo et al., 2017). In this study, we apply the analysis to a location off Albany on the south coast of western Australia, an area well-known for almost continuous exposure to long period swells. We use Australian Department of Transport (DOT) wave buoy data measured in 60 m of water over the period 2009 – 2017. The hourly data is close to continuous but contains some gaps corresponding to ~ 13% of the total duration, these are patched to form a continuous wave record.

Having sized the machine based on mean wave period, extreme wave height statistical analysis is performed using storm-based identification and a peaks-over-threshold technique, following Santo et al. (2016b), providing information relevant for any wave energy converter at the location. From operability and power scheme economics, we then compare the optimal size of machine, practical power output and the associated variability in power produced by an M4 machine at Albany to the open North Atlantic location off the Orkneys. This is performed with the methodology outlined in Santo et al. (2016a). For survivability, it is important to identify extremes of machine motion. Hence, extreme responses are also compared for the central hinge angle of the machine in survival mode with the power take-off turned off. We find that a much larger machine is required at Albany, because of the longer waves compared to Orkney. However, at the two very different locations the power/cost ratios are similar.

1. Introduction

This paper presents a complete analysis of a wave energy converter (WEC) from operability to survivability and the feasibility in terms of cost/power. We use the M4 machine as the WEC, which is a system with three floats in this study, each float is a vertical circular cylinder with a lower hemispherical end. The two smaller floats are rigidly connected by a beam above the water, and the largest float is connected to the mid float by a second beam; this is rigidly connected at the third and largest float but hinged at the middle float. The machine's power converter generates power through the relative angular motion of the hinge above the middle float. Thus, the complicated mechanical components are in the air, only the 'dumb' floats run below the water surface. To maximise the angular motions and hence the power generation, the spacing between each float is chosen to be about half a wavelength at the optimal operating condition; so the machine fits within a wavelength. The machine is single point

* Corresponding author.
E-mail address: harrif_santo@tcoms.sg (H. Santo).

https://doi.org/10.1016/j.renene.2019.06.146
0960-1481/

moored from the smallest float to a small mooring buoy through a cable and this buoy is then catenary moored to the seabed. Hence, the machine is self-aligning into the waves. The mooring system would also contain the cable for the transmission of the produced electrical power. The overall geometry of M4 is shown in Fig. 1, the dimensions correspond to laboratory scale (see Refs. [6,17] and the machine size is Froude-scaled into the field. For details of the design principles of the M4 machine, see Ref. [26]. There has been on-going development to look into different geometries and multi-float configurations as described in Ref. [25]. In this analysis, we use the same 'classical' M4 wave energy converter model as described in Ref. [19].

As far as we are aware, there are no available studies which report a complete analysis of a WEC from operability to survivability. Some studies concentrate on the operability in terms of practical power output and costing, while some focus on the survivability analysis of WECs. For example, the practical wave power generated by the Pelamis machine has been previously studied by Ref. [10] together with its associated power variability, while [2] provide a comprehensive numerical analysis for eight other WECs with different working principles. Extreme response statistical analysis is useful to determine the probability of any wave energy converter surviving extreme sea conditions. There are published studies looking into the effects of extreme responses on the mooring lines, but there are only few studies on the statistics of the extreme response of the device itself, e.g. see Refs. [1,11–13]. [5] provide a comprehensive survey on the survivability analysis of WECs in recent years. Meanwhile, there is growing number of studies looking into the hydrodynamics of the extreme responses of point absorber type WECs, all single float designs, using numerical Computational Fluid Dynamics (CFD) which are then compared with the physical experimental results, for example [4,14,15,22,30]. However, collecting response statistics by running CFD is extremely computationally intensive.

This paper is a continuation of our previous work looking at extreme wave height statistics, and subsequently the operability and survivability of the M4 machine in the northeast North Atlantic and North Sea, including Orkney, north of Scotland. This is the location of the European Marine Energy Centre (EMEC) test site, see Refs. [17,19,20]. Here we conduct similar analysis for Albany (on the south coast of Western Australia), providing extreme wave height analysis which is relevant for survivability of any WEC at the location, practical wave power analysis which is important from operability and power scheme economics, and subsequently extreme machine response analysis in which the M4 machine is in survival mode with power take-off turned off.

2. Discussion on locations, general metocean characteristics and type of data

Fig. 2 shows the locations of Albany and Orkney, with their zoom-in insets taken from http://www.transport.wa.gov.au/imarine/albany-tide-and-wave.asp, and http://www.emec.org.uk/about-us/our-sites/, respectively. For the location of Orkney, we assume that M4 is located at the EMEC 'full scale wave site, Billia Croo, 2 km west of the mainland of Orkney, in 60 m depth of water (tie-in points there vary from 50 m to 70 m). For the location of Albany, https://www.wawaves.org is another website providing data from wave buoys off Western Australia, including one recently installed in Torbay, close to Albany. The data provided on this website is from a Datawell buoy moored in 30 m of water approximately 1 km off the beach, installed as work in the Wave Energy Research Centre at the University of Western Australia and funded by the WA Government. The DOT buoy which has provided the 8-years of data that we have used in this work is in 60 m of water approximately 15 km off the beach. The assumption of our work is that M4 would be directly offshore of the Albany Wind Farm in 60 m depth. The Albany Wind Farm is located on the top of the cliff in the Torndirrup National Park, as shown in the subsequent photos.

Fig. 3 shows two photographs from the cliff top at Albany where a row of turbines in the onshore wind farm is visible in the right photograph.

Fig. 4 shows the comparison in terms of significant wave height (H_s), wave energy period (T_e), and mean wave direction at the two locations. Visual inspection of the two wave records shows some interesting differences. Albany is known for its exposure to long-period swells from the southern Indian Ocean and Southern Ocean, and there is relatively little variability nor seasonal variation throughout this wave record. Orkney on the other hand, being exposed to large waves from the open north east North Atlantic, is more variable, with both substantially larger extremes and smaller lulls in wave activity than the Albany record. Seasonality is also more marked in the North Atlantic. It is thus of interest to compare and contrast the performance of the M4 machine in these two rather different wave environments. Table 1 provides comparison of basic properties between the two sites.

We consider wave buoy data measured in 60 m of water at a location off Albany (S 35°2′1″, E 117°53′33″), so off the south coast of Western Australia. The data was downloaded from the Australian Department of Transportation (DOT) website. The buoy data records, provided at intervals of 15 min to several hours, contain information such as significant wave height (H_s), peak spectral period (T_p), mean wave period (T_m), and mean wave direction for total sea,

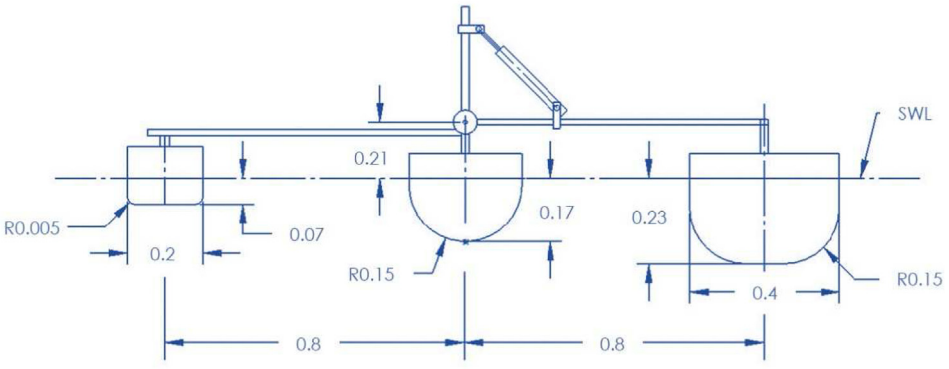

Fig. 1. Schematic diagram of the M4 wave energy converter (at laboratory scale, with dimensions in metres).

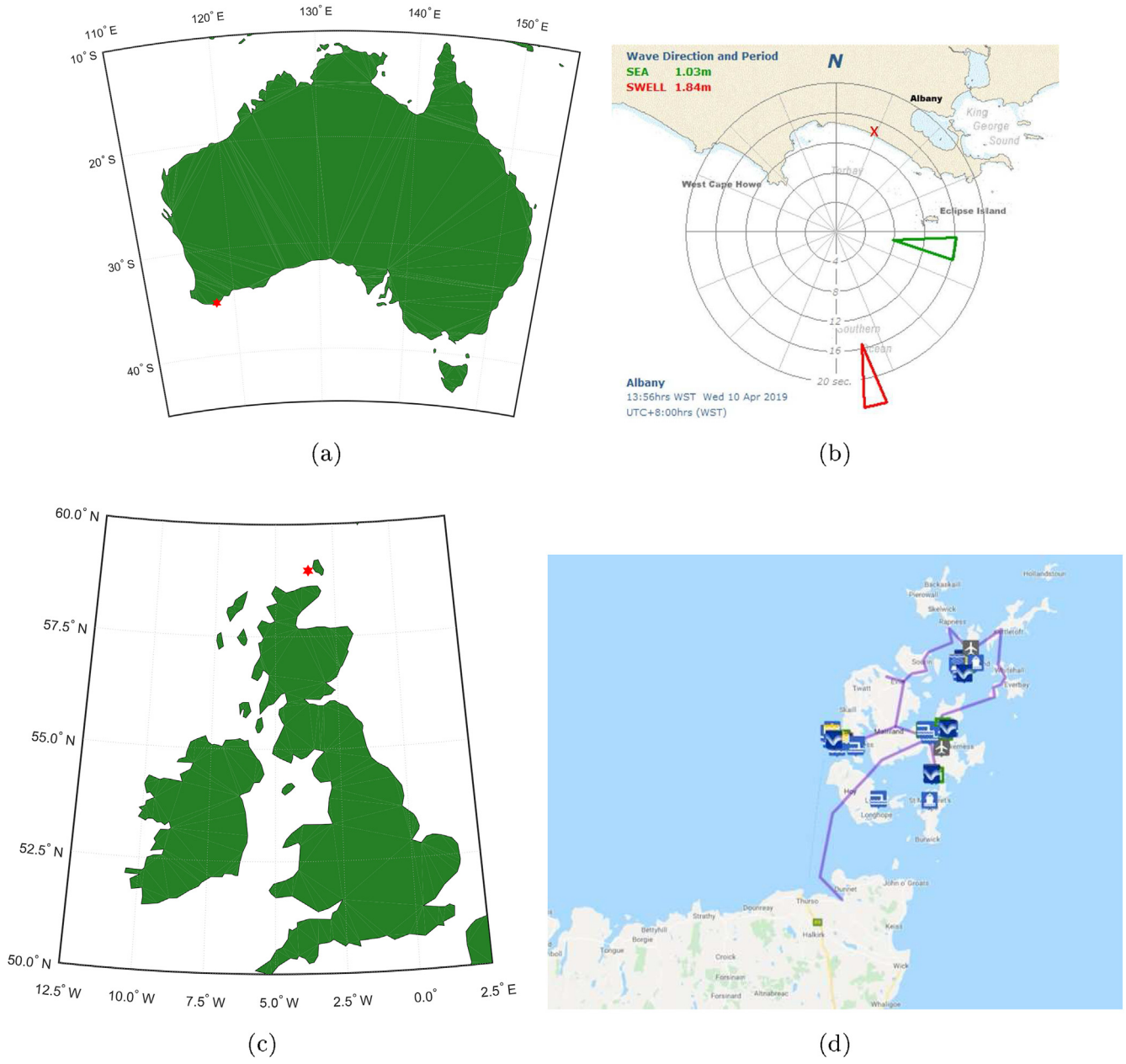

Fig. 2. Maps of (a,b) Albany and its zoom-in inset with the location of the onshore wind farm denoted with (red) cross, and (c,d) Orkney and its zoom-in inset. (For interpretation of the references to colour in this figure legend, the reader is referred to the Web version of this article.)

as well as wind sea and swell. The spectral components are also available for both wave energy and direction, but the spectra are truncated at 4 s (lower limit) and 28.6 s (upper limit).

The buoy data spans from 31 Aug 2008 to 15 June 2017, and for the analysis we use the data from 15 Jan 2009–14 Jan 2017, so a total of 8 complete years, Australian summer to summer. The data is close to continuous but contains some gaps corresponding to ∼13% of the total duration. The data of various intervals is first mapped into hourly data (or sea-state), by taking an average over the range of data that falls within the same hour. The gaps are then patched by assuming that, if the climate is varying across the gaps with the season, half filling (mirroring) from either side of each gap would approximately bridge the gap. In the analysis we choose to use the spectral components instead of the summary statistical quantities to avoid making an additional assumption on the shape of the wave spectrum. Due to the truncation, the statistics from the integral of the spectral components are ∼ 10% lower. However, given the characteristics of the M4 machine, this loss of very long and very short spectral components makes no difference to either the power take-off or survivability assessment.

The wave data at a location west of Orkney (N 58°58′12″, W 3°36′0″) is taken from the hindcast Norwegian 10 km Reanalysis Archive (NORA10) from 1958 to 2011, for more information see Ref. [16]. The hindcast wave data were available at 3 h intervals, and contain information such as date, time, significant wave height (H_s), peak spectral wave period (T_p), wind speed, wind and wave directions. Comparisons between hindcast and measured buoy data were conducted previously in terms of the significant wave height and period, H_s and T_p, at Haltenbanken (N 65°21′36″, E 7°8′24″) and Forties (N 57°47′24″, E 0°52′48″), and in general the agreement is good with no bias and with relatively small variability [21].

Some discussions on the two different sources of data are briefly

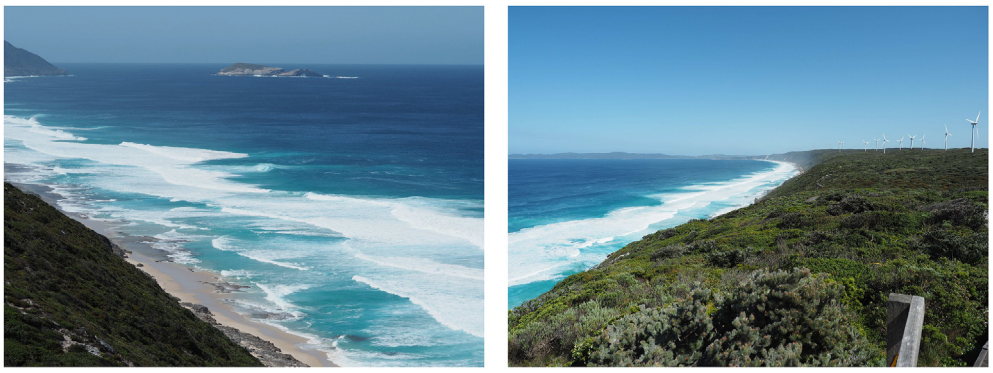

(a) (b)

Fig. 3. Views from the cliff-top above the assumed location of the M4 machine. Left photograph shows the view to the east from just below the eastern end of the onshore wind farm showing rock islands to the east. Right photograph shows the view to the west where a row of the turbines in the wind farm is visible. Photographs courtesy of P. H. Taylor.

provided as follows. Buoy or other type of measured data tends to span over short periods (a few years) and suffer from gaps/missing data due to intermittent discontinuity in the measurement. Hence, assumptions are required to patch the gaps and the uncertainty arising from that will affect the analysis. Also, the short duration of measurement data prevents meaningful analysis on the extreme value, in particular since any decadal or longer (climatic) variability, if it exists, will not be adequately captured. Nevertheless, measured data is 'real as much as any measurement is 'real – assuming the buoy characteristics are properly taken into account. Hindcast data, on the other hand, tends to span over longer period of time and to be continuous in record. However, since they are numerically simulated, from time to time the accuracy (and bias) has to be verified with ground truth measurement such as buoys/satellite.

3. Extreme wave statistics

For the extreme wave height analysis, the statistical analysis is performed using a storm-by-storm approach and a peaks-over-threshold technique, following [20]. The motivation for the storm-based statistics is that successive H_s values are strongly correlated, as they are likely to be part of a single longer storm. We perform analysis based on data for the whole year and then the 6 winter months only (May to Oct at Albany).

For the storm-based identification, two assumptions are required. First is on the storm cut-off value which is set at $0.8 \times H_{sMax}$; we use this threshold to define a single storm. Second is on the duration of the storm. Previously in Ref. [20], a single storm at a fixed location was assumed to last not more than 24 h, a reflection of the timescale for the motion of winter depressions in the north-east Atlantic and the North Sea. To assess whether this same assumption is suitable for Albany, we compare the average shape of the storm records containing the 25 largest H_s values in time for Albany and Orkney as shown in Fig. 5. It can be observed that for a cut-off at $0.8\times H_{sMax}$, the average storm duration is $\sim$ 17 hours for Albany and $\sim$ 10 hours for Orkney. Hence, the assumption of a maximum storm duration of 24 h is also applicable for Albany. The absence of the fast rise to the localised peak for the average storm history at Albany is presumably because storm centres and hence the most intense wave fields typically pass further south in the Southern Ocean. Albany has more of a swell environment. In contrast, Orkney is exposed to the most severe winter storms in the eastern North Atlantic with at least some of the storms tracking in a north-easterly direction towards the north of Scotland and passing directly over the Orkney Islands.

Once all storms have been identified, the most probable largest individual wave in each storm (H_{mp}), as first introduced by Ref. [28] using convolution integrals, can be estimated. This is a better parameter than H_{sMax} for each storm as it incorporates both the severity and duration. We follow the same procedure as outlined in Ref. [20] which is based on a simpler method using random sampling, assuming a Rayleigh distribution to account for the short-term variability of individual wave heights within a sea-state. Fig. 6 compares the distributions of H_{mp} for Albany and Orkney. In general, the H_{mp} values for Orkney are significantly larger than those for Albany. Both distributions tail off asymptotically towards the extremes, with Orkney apparently having a broader and more slowly decaying high tail as well as larger values.

The identified storms are ordered in terms of H_{mp} magnitude, and the peaks-over-threshold technique is used for the long-term extrapolation. In this analysis, we assume that the exceedances (observations above a threshold) can be fitted into the class of 'thin' asymptotic tails with a Weibull distribution form, with the cumulative density function written as:

$$P = 1 - \exp\left[-\left(\frac{H_{mp}}{\alpha}\right)^{\beta} + \left(\frac{H_c}{\alpha}\right)^{\beta}\right] \quad (1)$$

where H_c is the minimum cutoff (threshold) value of H_{mp} used in the fit, α and β are the scale and shape parameters, respectively, to be obtained by the maximum likelihood method.

Robust threshold behaviour is important for POT analysis. We investigate the sensitivity of the extrapolation to the threshold level by using the number of storms downwards from the most severe as a threshold, and find that a threshold value of about 400 largest storms for 8 years of data is appropriate. This corresponds to about 50 storms per winter, roughly 2 per week. This criterion works well for both Albany and Orkney (noting that the Orkney wave data is 54 years long and a threshold of 1000 largest storms is used here). Fig. 7 (a) shows the long-term fit of the H_{mp} for Albany using the entire record, and just the winter data (May–Oct). Every data point (crosses) represents an individual storm severity (H_{mp}) from the buoy data, while the lines are obtained by a non-parametric bootstrap. Since there is still some, although relatively weak, seasonal variation within a year in Albany, there is only a very small difference between the fits to the winter data alone and that for the whole year. We also investigate the fit of the exceedances with a variant form of Weibull distribution as described in the Appendix. Comparable results are obtained, demonstrating that the results from the long term extrapolation are robust. Fig. 7(b) shows the fit for the Orkney Islands location. All the wave heights are larger and the Weibull fits are now straight lines on the plot, so the

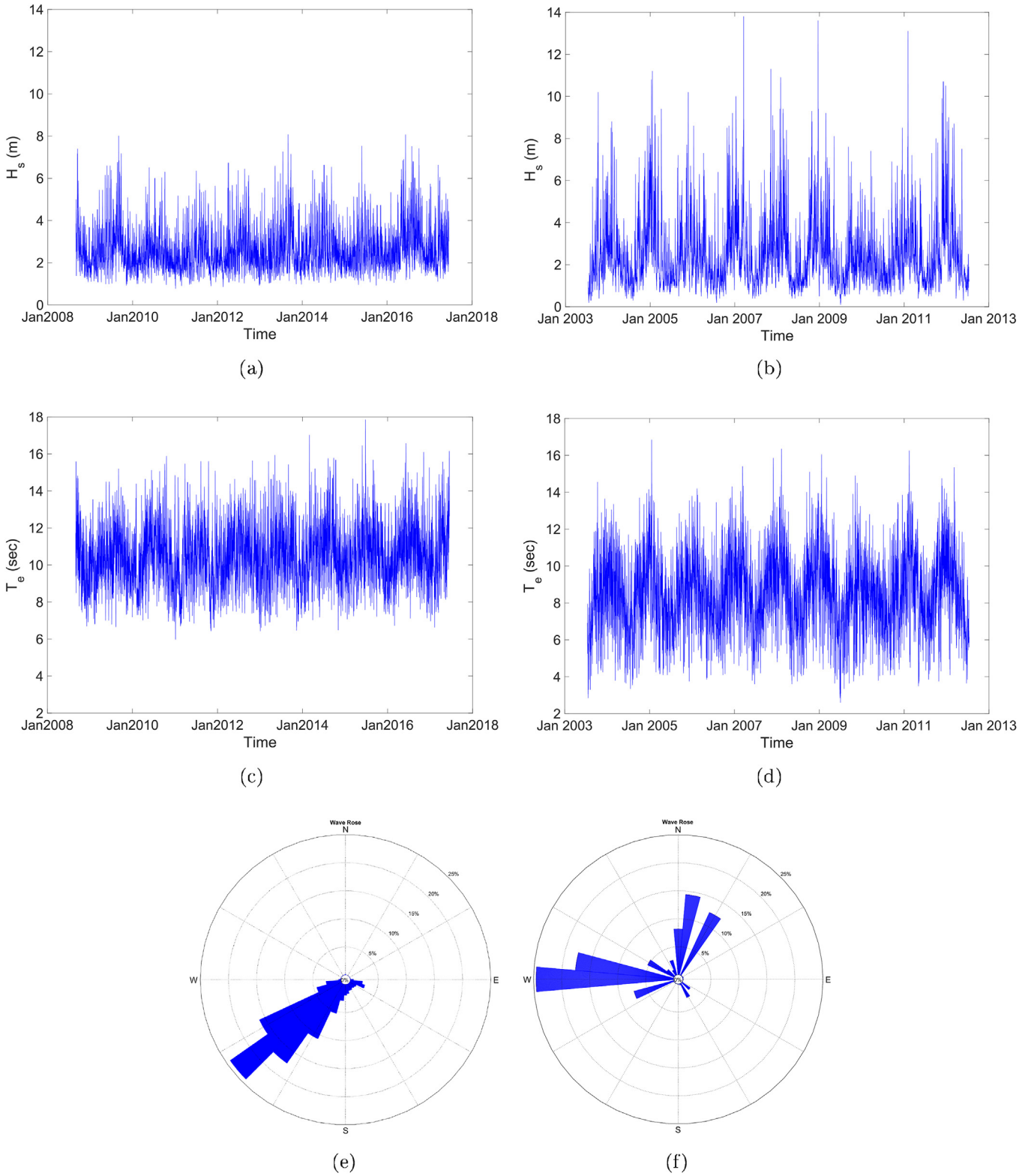

Fig. 4. Comparison of (a,b) H_s, (c,d) T_e and (e,f) wave direction between Albany (left) and Orkney (right).

Weibull form reduces to a simple exponential tail. At long return periods, this implies a much wider high tail and thus much larger waves at Orkney. Confidence intervals (5–95%) are approximated by simple bootstrapping. The original fit forms and the mean of the bootstrapped results match well.

Table 2 compares the extreme wave heights for Albany and Orkney. Extreme waves at Albany are considerably less severe than Orkney, and in general anywhere in the exposed eastern North Atlantic and North Sea, particularly at return periods of 1 in 100 years and upwards. It is worth noting that the wave height (H_{mp})

Table 1
Comparison of the basic properties between Albany and Orkney.

Properties	Albany	Orkney
Water depth (m)	60	assumed 60 (ranging from 50 to 70 m)
Distance to shore (km)	15	2
Time period of data for analysis	15 Jan 2009–14 Jan 2017 (8 years)	15 Jul 1958–14 Jul 2012 (54 years)
Average (and std) H_s (m)	2.87 (1.05)	2.93 (1.57)
Average (and std) T_p (s)	12.91 (1.99)	11.54 (2.65)

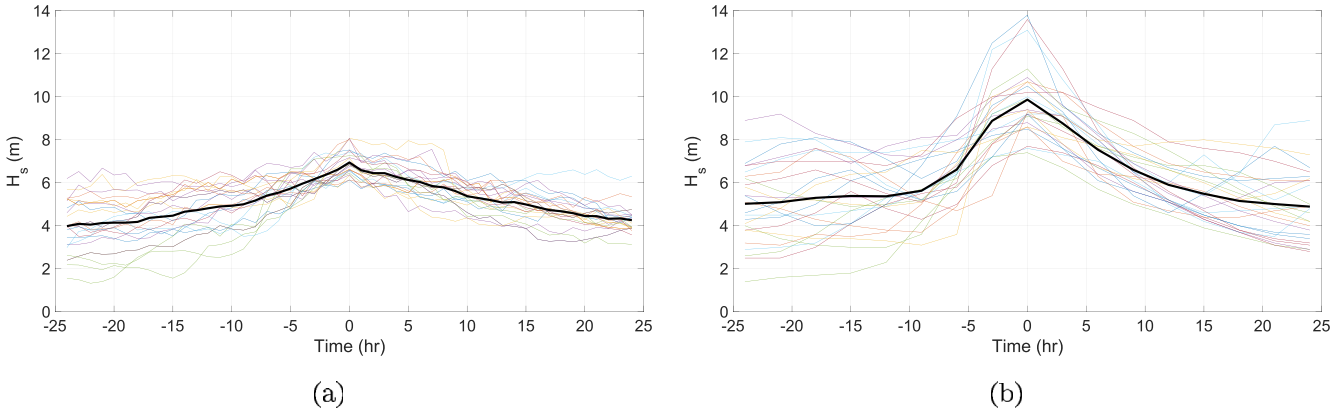

Fig. 5. Comparison of the average shape (thick black line) of the 25 largest H_s in time between (a) Albany and (b) Orkney.

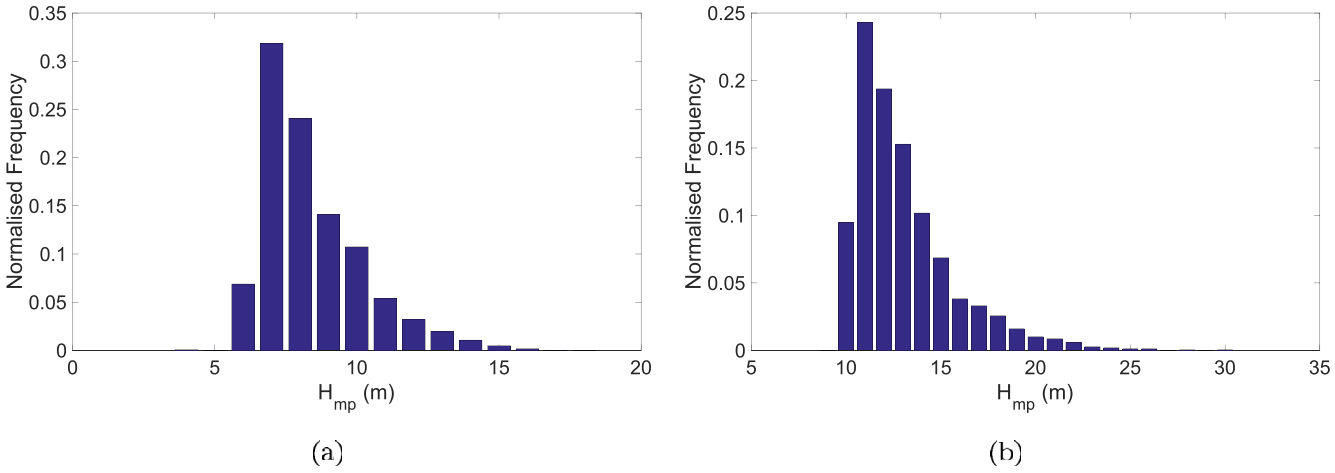

Fig. 6. Comparison of the distribution of H_{mp} between (a) Albany and (b) Orkney.

ratios shown in same table are stable in that other (thin) tail forms would give the same values. We have repeated the POT analysis using the individual H_{sMax} values as a measure of storm severity. The results are also given in Table 2. The fits are equally good as those for H_{mp}, with values close to a factor of 2 smaller. This factor between the most probable maximum individual wave, H_{mp}, within each storm and the H_{sMax} value for that storm is consistent with each storm containing a few thousand waves, and the use of the Rayleigh narrow-banded approximation for the distribution of wave heights within each storm.

4. Practical wave power by M4

Following the design recipe from Ref. [24] as used by Ref. [19]; the M4 machine is sized based on the long-term average energy period, T_e, of Albany, which is 10.5 s. This is substantially longer than anywhere in North East Atlantic and North Sea (with values ranging from 6 to 9 s), even for locations fully exposed to North Atlantic winter storms. Consequently, a larger machine size is proposed for Albany, giving an overall machine length of 146 m using the standard sizing recipe. In comparison, the machine size for Orkney (EMEC) is 94 m, so about $2/3\times$ size.

To estimate the practical wave power, the M4 capture width characteristics is required. We use the same capture width ratio (as a function of incident wave energy period) for a power take-off coefficient (PTO) of 3 Nms (at model scale) as described in Ref. [19]. This is based on the experimental results by Ref. [24] and numerical prediction from a coupled hydrodynamic-structural model by Ref. [6]. There is no account of directional spreading in this analysis, hence the assumption is that the waves are mostly close to uni-directional and that the M4 machine is pointing along the mean wave direction. Being restrained by a single point mooring to the smallest float, M4 is a self-aligning geometry with respect to wave direction.

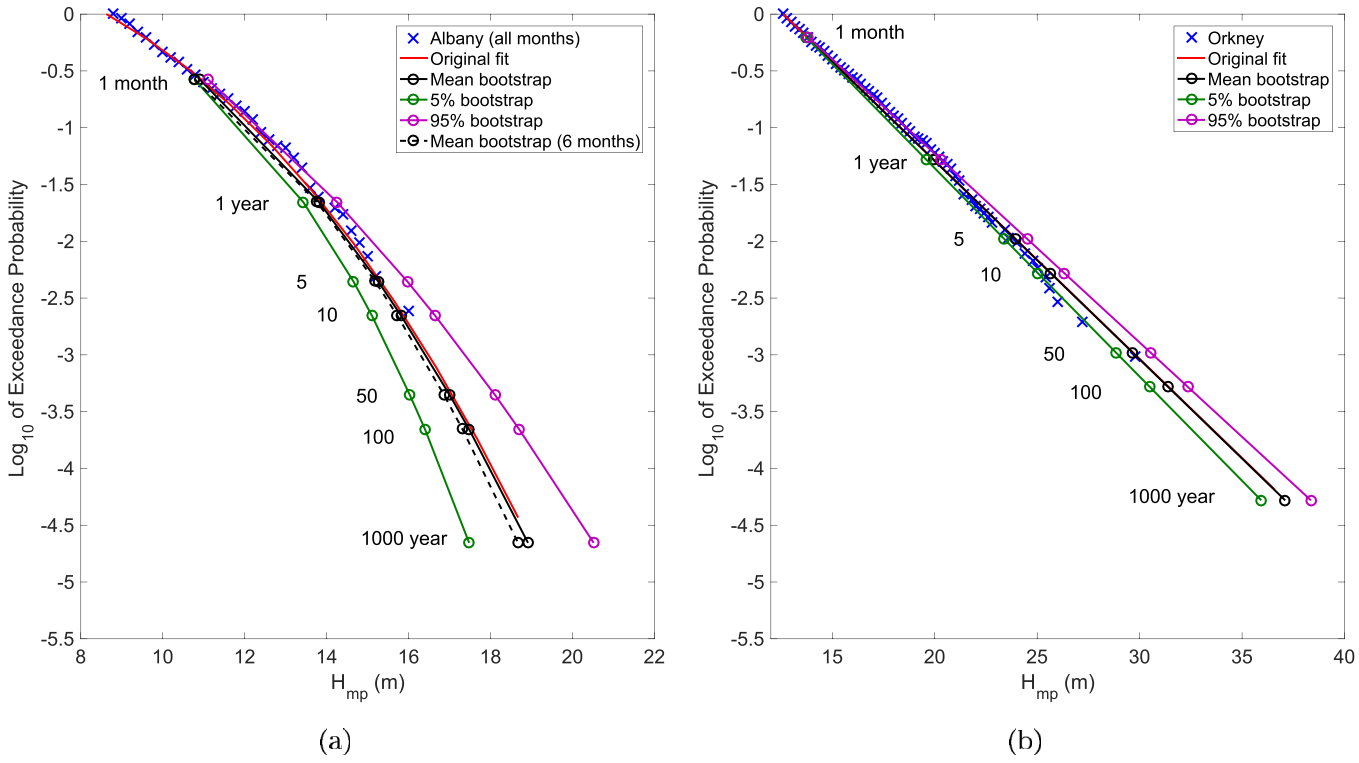

Fig. 7. Long-term extrapolation using Weibull fit for (a) Albany for whole year data (solid lines, $\alpha = 3.7$ and $\beta = 2.7$) and winter 6 months (dashed line, $\alpha = 4.0$ and $\beta = 2.9$), and threshold $N \sim 400$ largest storms, and for (b) Orkney with winter 6 months ($\alpha = 1.2$ and $\beta = 1.0$, hence a simple exponential fit) and threshold $N \sim 1000$ largest storms. The circles from bottom up correspond to H_{mp} with a return period of one in 1000 years, 100 years, 50 years, 10 years, 5 years, 1 year and 1 month, respectively.

Table 2
Comparison of the extreme wave heights between Albany and Orkney.

Extreme wave	Albany	Orkney
100-yr H_{mp} (m)	17.5	31.4
1000-yr H_{mp} (m)	18.9	37.1
Ratio	1.1	1.2
100-yr H_{sMax} (m)	9.4	16.2
1000-yr H_{sMax} (m)	10.4	19.2
Ratio	1.1	1.2

The wave power is computed using the integral of the spectral components. Since the location of the buoy data does not satisfy a deepwater condition, an additional correction to account for water depth effect is incorporated into the wave power estimation, e.g. see Ref. [23]. The methodology to obtain the practical wave power on a sea-state basis is briefly as follows:

1 Compute the power on a sea-state basis (H_s, T_e) incorporating the capture width characteristics and assumed mechanical efficiency of 0.9.
2 Obtain the average practical power over 8 years of data. This is termed the “no clipping” case.
3 Assume the machine capacity = 3× long-term average practical power, so power output saturates if the practical power in any 1-h interval exceeds this capacity. This is termed the “power clipping” case.
4 Re-compute the average practical power including clipping until convergence.

We note the use of the wave energy period (T_e). This is computed from integrals over the measured spectrum for Albany. For Orkney, this was estimated as $T_e = (T_p + T_z)/2$ [19].

Fig. 9 shows the annual average wave power at Albany and Orkney over 8 years of data. As well as the practical wave power which is obtained using the capture width ratio, an idealised practical wave power is obtained by incorporating a flat frequency-independent capture width ratio, matching the peak value of the practical capture width ratio (0.4, see the dashed line in Fig. 8). This represents a physical limit of energy capture for the machine (in terms of length of crest). The ideal practical wave power can then be used to define a power output efficiency. The long-term average of the practical wave power at Albany is just below 1 MW, with a power efficiency of 57%. In comparison, the equivalent power at Orkney (with a size 2/3× smaller) is 319 kW and a power efficiency of 34%. We note also the larger relative variability year on year at Orkney, in particular in terms of the ideal practical wave power (coefficient of variation (CV), defined as the ratio of the standard deviation to the mean, is 11% for Orkney and 7% for Albany). This is consistent with the Albany wave environment being more swell dominated.

Based on operability and power scheme economics, and the standard Stansby design recipe for M4, Albany is a little more attractive location compared to Orkney. With an Albany machine 1.55× larger than Orkney, power/cost is 1.3× better for Albany than Orkney if cost ∼ length^2, and close to identical if cost ∼ length$^{2.5}$. The requirement for machine survivability, however, may lead to different conclusions, and this is assessed in the next Section.

5. Extreme response statistics

For the extreme response statistics, we perform statistical analysis in terms of the peak hinge angle, assuming the PTO is switched off and the machine is in survival mode. For the present M4 machine configuration with a straight beam connecting the middle float and the largest float, the limiting angle before self-

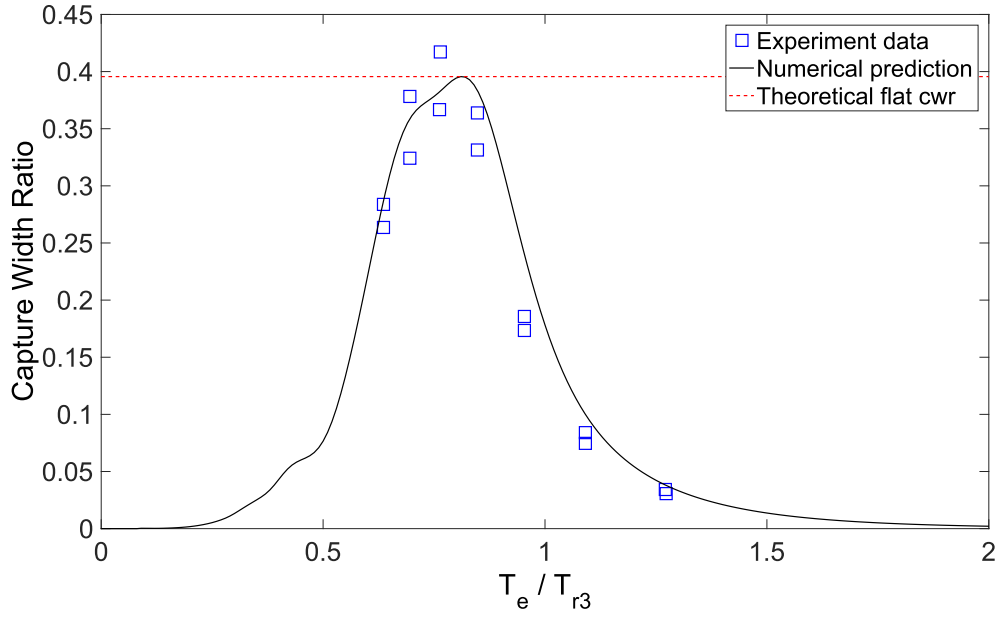

Fig. 8. Plot of capture width ratio variation with ratio of energy period to heave period of stern float (T_e/T_{r3}) for power take-off coefficient (PTO) of 3 Nms (at model scale). Experimental data are taken from Ref. [24]; and the numerical prediction is from Ref. [6]. The dashed line is the theoretical flat capture width ratio used for assessment of the ideal practical wave power, where the capture width at the peak is taken as a representative reference.

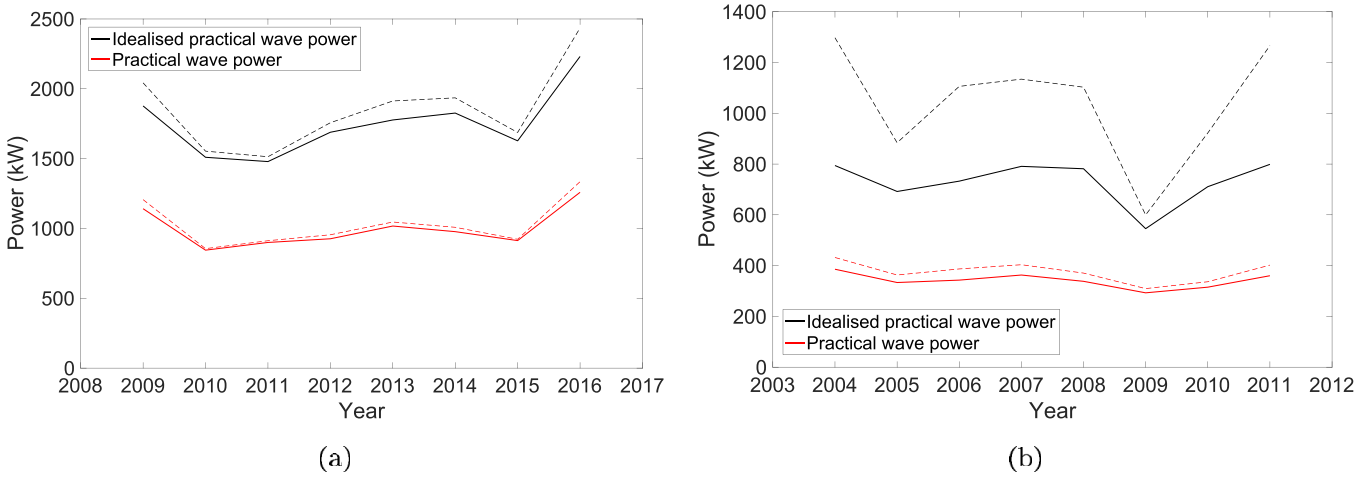

Fig. 9. Annual mean ideal practical and practical wave power at: (a) Albany and (b) Orkney (b, for an equivalent 8 year period). Dashed lines are the power output without saturation (no clipping), solid lines with saturation (clipped at 3× long-term mean power).

collision between the middle float and the beam is $\sim 40^\circ$, which we assume governs the survivability requirement. This does implicitly assume that mooring design is sufficiently mature to provide a suitable system for any conditions. It is thus important to assess whether the M4 sized for Albany in the previous section also satisfies the survivability requirement.

Fig. 10 presents scatter diagrams of normalised occurrence of H_s and T_p for the entire 8 years of record at Albany and entire 54 years of record at Orkney, with red indicating the highest number of occurrences. The two lines represent lines of constant steepness (defined as $s = H_s/T_p^2$): solid line for the constant limiting steepness ($s = 0.0584$ for Albany), and dashed line for the constant mean steepness ($s = 0.0149$ for Albany). The limiting steepness line in one sense represents the most severe historical sea-states ever predicted at that location during the period of the available data. In comparison, the constant limiting steepness and constant mean steepness for Orkney is $s = 0.0576$ and 0.0169, respectively. As could be anticipated, the limiting wave sea-state steepness at both locations is virtually identical - and presumably limited by wave breaking. In contrast, the average wave steepness at Albany is slightly lower than for Orkney and the average period is also significantly larger. Also shown is the long-term mean T_e of Albany represented by a straight vertical solid line. It can be seen that the diagram is dominated by waves with periods greater than 8 s, indicating that Albany is dominated by long-period swells. Also, the mean T_e which is used to size the machine is considerably closer to the periods with the highest number of occurrences, indicating that the machine response is likely to be large.

Following [17]; we perform linear response statistics for survivability of the M4 machine in severe sea-states, assuming the power take-off is disconnected. Linear statistics is assumed, neglecting the effect of nonlinearity due to local submergence of the floats ('dunking') and possibly viscous damping for very large relative motion. Including the effect of this nonlinearity will reduce

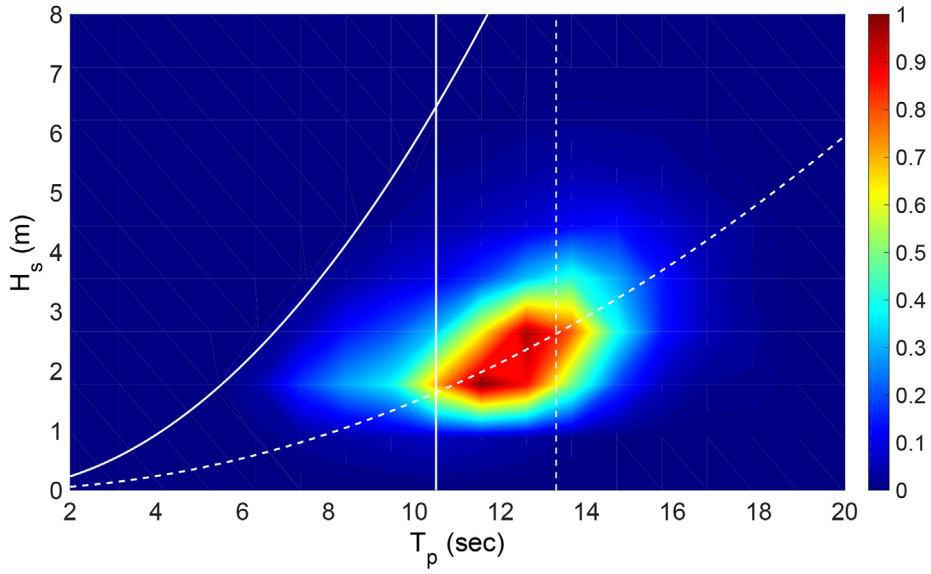

(a) Albany

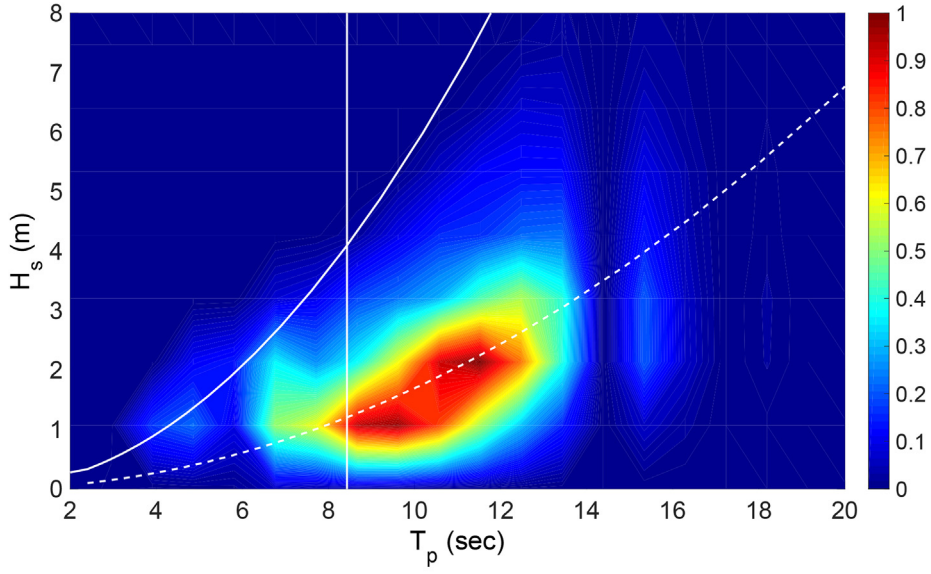

(b) Orkney

Fig. 10. Scatter diagrams of normalised occurrence of H_s and T_p at (a) Albany from 2009 – 2016 and (b) Orkney from 1958 – 2012. Red region indicating the highest number of occurrences. Solid line represents the constant limiting steepness, dashed line represents the constant average steepness and a straight vertical solid line represents the long-term mean T_e which is used to size the M4 machine. An additional dashed vertical line for Albany represents the optimum size for Albany which is 1.6× the standard machine size which is based on long-term mean T_e. (For interpretation of the references to colour in this figure legend, the reader is referred to the Web version of this article.)

the peak response in general, though we note that laboratory tests on an M4 model show that the machine motion is remarkably linear. The overall damping with the PTO disconnected is almost entirely due to wave making by the moving machine, until the motion is so large that the central float starts to 'dunk'. Hence, these linear results give an upper bound on machine responses.

To obtain the machine response for each sea-state, we convolute the same machine Response Amplitude Operator (RAO) as in Ref. [17] with the spectral components. We perform the analysis assuming two different models for wave spreading in the sea-states: uni-directional, and directional sea-state using bimodal directional spreading in fetch-limited sea-states following [7]. We assume that the machine always points into the mean wave direction. It is worth remarking that the sea-state in Albany is on average less spread than in Orkney, hence the use of Ewans spreading model could be slightly non-conservative, but the assumption of uni-directional waves will remain conservative.

Fig. 11 shows the histogram of the most probable maximum linear hinge angle for each hour in the dataset for Albany and for each 3 h period for Orkney, for both uni-directional and directional spread seas. The statistics are collected over the entire 8 years of record at Albany and entire 54 years of record at Orkney. It can be seen that the distribution for Albany is shifted to the right (towards larger hinge angle) relative to that for Orkney, indicating that the

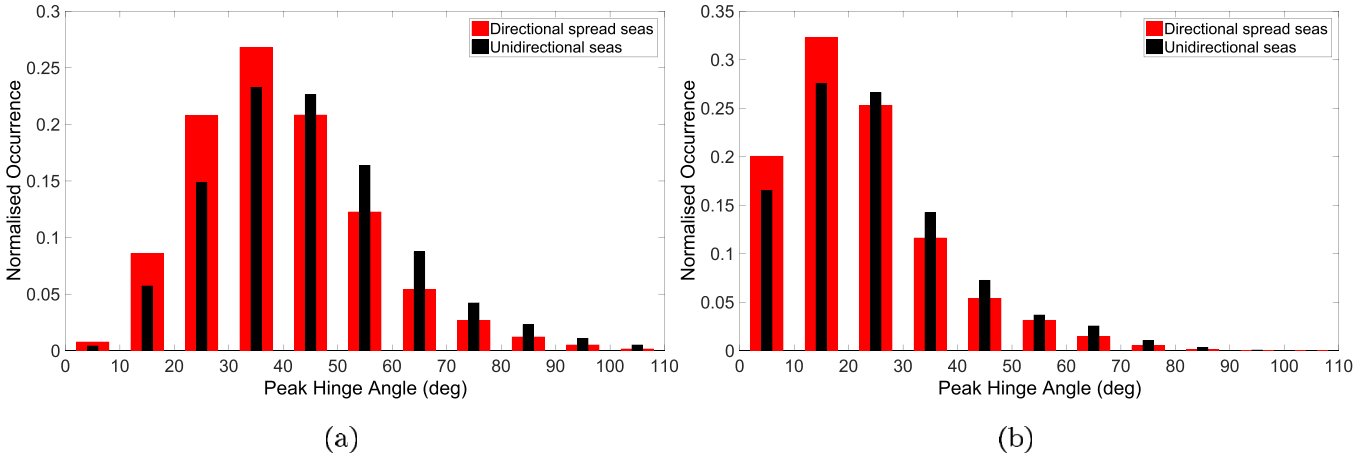

Fig. 11. Comparison of the histogram of the peak hinge angle distribution of the M4 machine sized for (a) Albany per hour and (b) Orkney for each 3-h interval with two different sea-state assumptions. The probability of a response level in each 10° bin is given by the height of the bar in that bin.

risk of self-collision of the beam between the centre and rear floats with the edge of the centre float is greater for Albany compared to Orkney. This can also be observed from the average time between occurrences of the hinge angle exceeding 40°, as listed out in Table 3. It can be seen that for the Albany-sized machine, the average time is only 2–3 h compared to that for the Orkney-sized machine which is about 20–28 h. Thus, from survivability perspective based on linear analysis, the present machine sized for Albany based on the standard Stansby design recipe with a straight beam is liable to self-collision.

Given the size difference between Albany and Orkney, it is of interest to investigate how the M4 machine of Orkney size might perform in Albany. The analysis is repeated with the machine size × 1.5 smaller (to match an Orkney-sized machine), as well as 1.6× larger, and the histograms are shown in Fig. 12. The risk of self-collision is decreased by up-sizing the machine, while down-sizing the machine will increase the risk of self-collision instead. This is counter-intuitive to the initial assumption that a smaller machine will ride over the crests and troughs of the long waves, but for large amplitude and long peak period storms there will always be a high frequency tail of the wave spectrum providing combinations of shorter waves that will excite the smaller machine more than the larger machine. Increasing the size of the machine causes the machine to react less to the shorter waves within the same sea-state. The scaled up Albany machine (length 234 m, 1.66 ×) has very similar hinge rotational statistics to the original Orkney machine (with a length of 94 m), though it would be more expensive to construct and would produce substantially more power.

5.1. Designer waves

Here we present comparisons of the wave and machine responses in time for a 1 in 1 h sea-state for Albany and 1 in 3 h sea-state for Orkney. H_s is chosen to be 1 in 10 year return period, which corresponds to 8.4 m for Albany and 13.5 m for Orkney. The associated T_p is chosen from the limiting steepness lines and the mean steepness lines (from the scatter diagrams). The machine response is presented for the optimally sized machine for each location, i.e. 234 m long for Albany and 94 m long for Orkney, respectively. Since the high frequency spectral tail components are truncated from the buoy data for Albany, we assume a JONSWAP spectral shape with peak enhancement factor of 3.3.

We present several results on average shapes of extreme waves and machine responses in these hypothetical storms. We examine the shape of the most probable maximum wave (crest) shape in time, and the predicted machine response due to that wave. We also present the time history of the most probable maximum machine response in time, and the input wave group which would produce this machine response - the designer wave. All of these are based on the same sea-state. The average shape of an extreme response in a linear random Gaussian process (NewWave) is proportional to the auto-correlation function for that process, see Refs. [8,9,29] as well as [20] for application to M4. The magnitude of the peak response crest can be determined using the Rayleigh distribution of peaks in the random field. The equations of the auto-correlation functions for wave (crest) and machine response are briefly provided as follows.

Table 3
Comparison of the long-term mean peak hinge angle between Albany and Orkney.

Location and type of sea-state	Mean of the peak hinge angle distribution (deg.)	Average time between occurrences of the hinge angle exceeding 40 deg. (hr)
Orkney (machine length 94 m)		
Unidirectional	24.5	20
Directional	21.7	28
Albany (machine length 146 m)		
Unidirectional	44.5	2
Directional	39.4	3
Albany (machine length 94 m)		
Unidirectional	56.8	2
Directional	49.0	2
Albany (machine length 234 m)		
Unidirectional	19.8	13
Directional	16.7	29

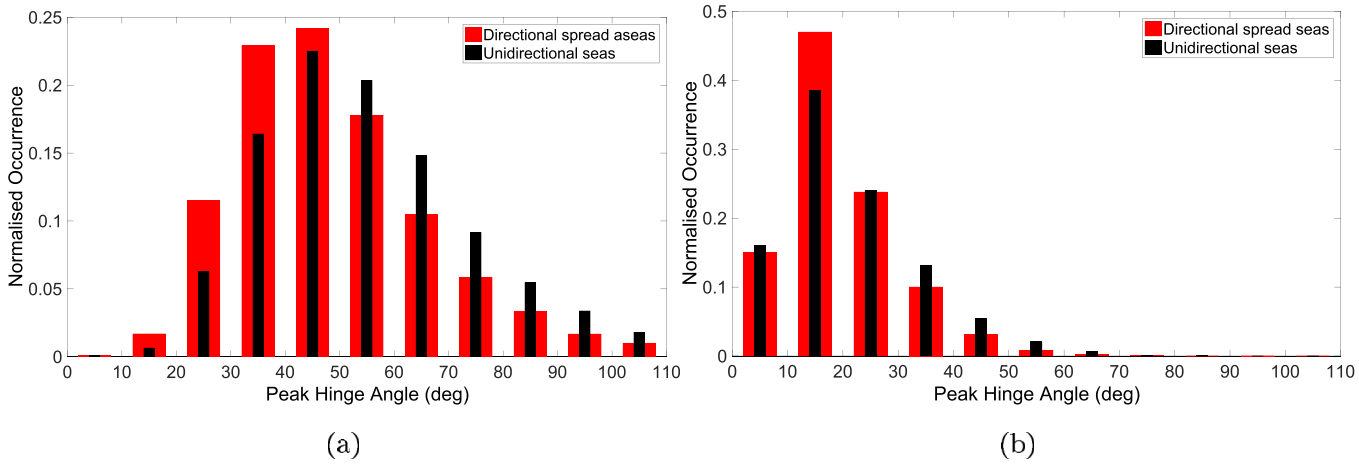

Fig. 12. Comparison of the histogram of the peak hinge angle distribution of the M4 machine for Albany which has been sized (a) 1.5× smaller and (b) 1.6× larger relative to the original size. The probability of a response level in each 10° bin is given by the height of the bar in that bin.

The average shape of the largest waves in the incident random wave field, the NewWave in surface elevation, is expressed as:

$$\eta_{NW} = \alpha_\eta \frac{\sum_n S_{\eta\eta}(\omega_n)\Delta\omega \mathrm{Re}[\exp(i\omega_n t)]}{\sum_n S_{\eta\eta}(\omega_n)\Delta\omega}. \quad (2)$$

Demonstrations that this shape does match the average linear components of large wave crests (and troughs) in time are given in Refs. [8,27] for winter storms in the North Sea, and in Ref. [18] for Hurricane Camille in the Gulf of Mexico.

The associated response angle in time due to the NewWave in surface elevation is expressed as:

$$\phi_{\eta_{NW}} = \alpha_\eta \frac{\sum_n S_{\eta\eta}(\omega_n)\Delta\omega \mathrm{Re}[Z_{n\theta=0}\exp(i\omega_n t)]}{\sum_n S_{\eta\eta}(\omega_n)\Delta\omega} \quad (3)$$

where $S_{\eta\eta}(\omega_n)$ is the power spectrum of surface elevation, ω_n is the frequency of the n^{th} wave component, $Z_{n\theta=0}$ is the machine RAO for unidirectional waves, and α_η is the most probable maximum wave amplitude in N samples.

Equivalently, the average size and shape in time of extremes in the response angle, which could be termed as the NewWave in response angle, is simply:

$$\phi_{NW} = \alpha_\phi \frac{\sum_n S_{\phi\phi}(\omega_n)\Delta\omega \mathrm{Re}[\exp(i\omega_n t)]}{\sum_n S_{\phi\phi}(\omega_n)\Delta\omega} \quad (4)$$

The unidirectional designer wave as the wave time history which would give the NewWave in response angle can be defined as:

$$\eta_{\phi_{NW}} = \alpha_\phi \frac{\sum_n S_{\phi\phi}(\omega_n)\Delta\omega \mathrm{Re}\left[Z^{-1}_{n\theta=0}\exp(i\omega_n t)\right]}{\sum_n S_{\phi\phi}(\omega_n)\Delta\omega} \quad (5)$$

where $S_{\phi\phi}(\omega_n)$ is the power spectrum of the hinge angle response, and α_ϕ is the 1 in N linear crest elevation in the random sea-state. Both α_ϕ and α_η can be approximated for large N samples as:

$$\alpha = \sqrt{(2m_0 \log N)} \quad (6)$$

where m_0 is the total variance of the power spectrum for the wave field or the machine response, as appropriate. In general, N is obtained from the zero crossing period (T_z) of waves or responses in a 1 or 3 h sea-state. Further, we note that $S_{\phi\phi} = S_{\eta\eta}|Z_{n\theta=0}|^2$, because the M4 machine is assumed to behave linearly. Applying these results to both the incident wave fields and the M4 machine responses at Albany and Orkney, we obtain the following predictions.

The left hand column of plots in Fig. 13 show the shape in time of the most probable maximum (linear) wave crest (NewWave, η_{NW}) in 1 h (Albany) and 3 h (Orkney) sea-states; these are of course independent of the choice of the M4 machine. The centre column of plots show the response of the specified M4 machine to the left hand wave group. The right hand plots show the most probable maximum machine response in time (ϕ_{NW}) in the sea-state for the specified M4 machine. Due to the different machine sizes, the natural frequency of the M4 machine for Albany is different compared to that for Orkney. Previously [20] found that the most probable maximum machine response time histories along limiting steepness storms are very similar for Orkney (regardless of T_p since the response is governed by the form of the JONSWAP high tail), but this is not the case for Albany (where the machine resonant period is much closer to the peak wave period, T_p).

Discussing, in more detail, the centre column of plots in Fig. 13, this shows both the machine response in time given an input of the most probable maximum wave ($\phi_{\eta_{NW}}$, with time axis running left to right, and the vertical axis scale on the left), as well as the wave group (designer wave, $\eta_{\phi_{NW}}$, with the time axis running right to left, and the vertical axis scale on the right) which would produce the most probable machine response in time. The shape of these two functions, $\phi_{\eta_{NW}}$ and $\eta_{\phi_{NW}}$, are identical - a powerful and useful example of reciprocity for linear systems. It can be seen that there are some differences in the temporal shape of the designer waves between Albany and Orkney. Since the M4 machine for Albany has lower natural frequency (longer period), the wave frequency required to drive the most probable maximum response in time is also lower compared to that for Orkney.

With different size of machine (or different type of machine) responding to waves differently, the concept and the use of a designer wave, which is designed for each device, is useful to assess the survivability requirement, although qualitatively, the designer waves for survival for M4 machines at Albany and Orkney are similar. Of course the most extreme machine motions shown in Fig. 13 would threaten the survivability of the M4 machine. However, we note that previous physical testing in the Plymouth COAST laboratory wave showed that, for predicted rotation angles greater than $\sim 35^\circ$, the central float is temporarily submerged and this greatly limits the extreme motion of the machine [20]. Secondly, we observe that such severe sea-states, and storms, along the limiting

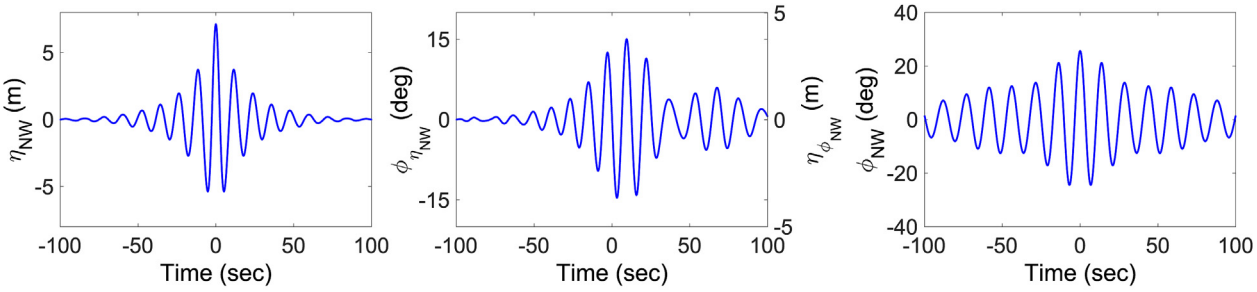

(a) $T_p = 12$ sec, $H_s = 8.4$ m, Albany M4, length 234 m

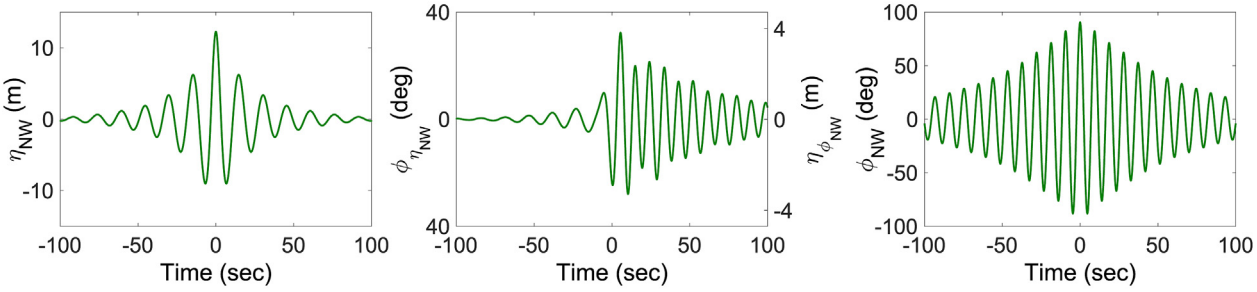

(b) $T_p = 15.3$ sec, $H_s = 13.5$ m, Orkney M4, length 94 m

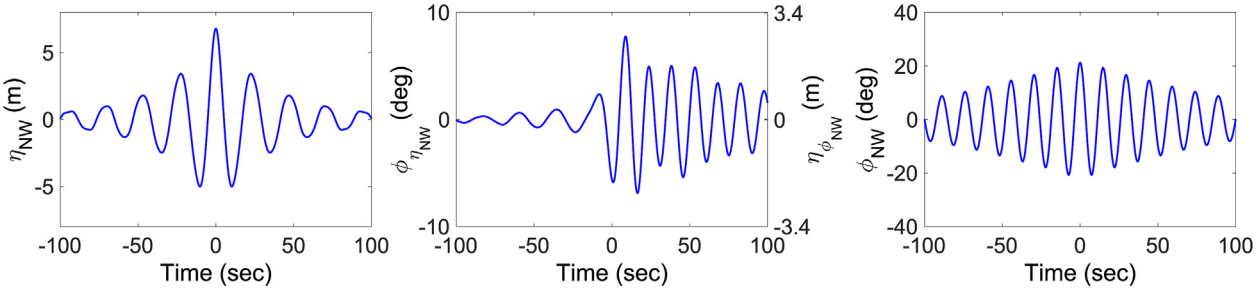

(c) $T_p = 23.75$ sec, $H_s = 8.4$ m, Albany M4, length 234 m

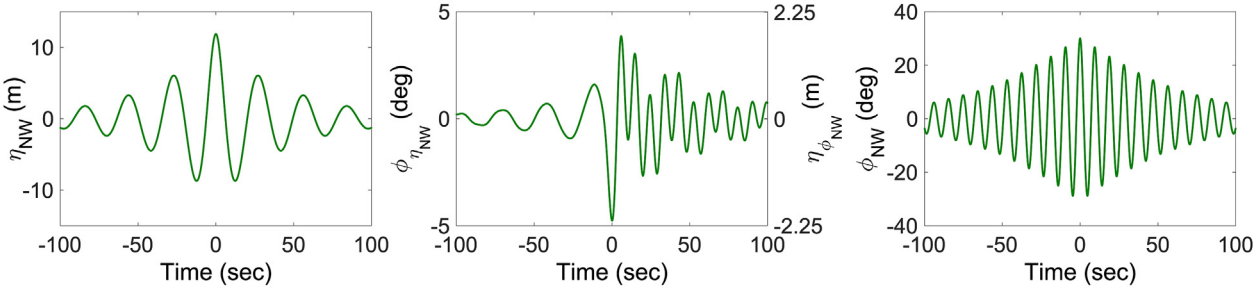

(d) $T_p = 28.3$ sec, $H_s = 13.5$ m, Orkney M4, length 94 m

Fig. 13. Plots of wave and machine response time histories for a 1 in 1 h sea-state for Albany and 1 in 3 h sea-state for Orkney, with the H_s chosen to be 1 in 10 year return period. The associated T_p is chosen from the limiting steepness lines for (a,b) and from the mean steepness lines for (c,d). Left hand column shows the shape of the most probable maximum wave crests for each sea-state (η_{NW}). Right hand column shows the most probable maximum response in time for each sea-state (ϕ_{NW}). Centre column shows the machine response given an input wave group matching the most probable maximum wave in time ($\phi_{\eta_{NW}}$), and also the wave group (with the time axis reversed) which would produce the most probable maximum machine response in time ($\eta_{\phi_{NW}}$).

wave steepness are very unlikely. However, these designer wave cases would be ideal as input conditions for full CFD simulations of short duration, as well as for experiments in a wave tank, each requiring only a few waves to be simulated as opposed to having to run long random wave simulations. Finally, we note that the relationships in Fig. 13, running horizontally, are linear. Hence, applying an arbitrary scaling to the size of the maximum wave crests (left), the same scaling applies to both the centre and the

right hand subplots for response given the wave, wave given the most probable maximum response, and the most probable maximum response itself.

6. Economic scaling of machine size

The results in Fig. 14 complete the analysis by looking at the variation from power output and peak hinge angle with respect to machine size and ultimately cost for both Albany and Orkney. Increasing the machine size up to 2× the original size will increase the power output, as shown in Fig. 14(a), and reduce the peak hinge angle, as shown in Fig. 14(b), beyond which the cost of building multiple originally-sized machines will be significantly cheaper than that for a single larger machine, as shown in Fig. 14(c). By doubling the machine size from the original/initial size, under the same increase of cost relative to the original size, the M4 machine at Orkney produces more additional power output (from the ratio of power to that of the original size) relative to Albany. However, the machine at Albany gains a more drastic reduction in the peak hinge angle relative to Orkney.

To assess whether the M4 machine is more cost-effective in Albany or Orkney, one has to investigate the results in terms of the power to cost ratio, as shown in Fig. 15. As obvious from the figure, for the original 1.5× machine size for Albany relative to the size for Orkney, the machine is more cost-effective for Albany. However, since the machine for Albany has to be up-sized to match the survival characteristics of the Orkney machine, this effectively pushes the power cost ratio in favour of Orkney. Our analysis suggests that the three-float M4 design can be sized to work well at each location, the size difference simply reflects the different characteristics of the wave fields at the two locations. We also note that continuing work on improved designs of M4-type machines could potentially produce more power per machine at significantly lower cost/power [25], albeit with increased machine complexity.

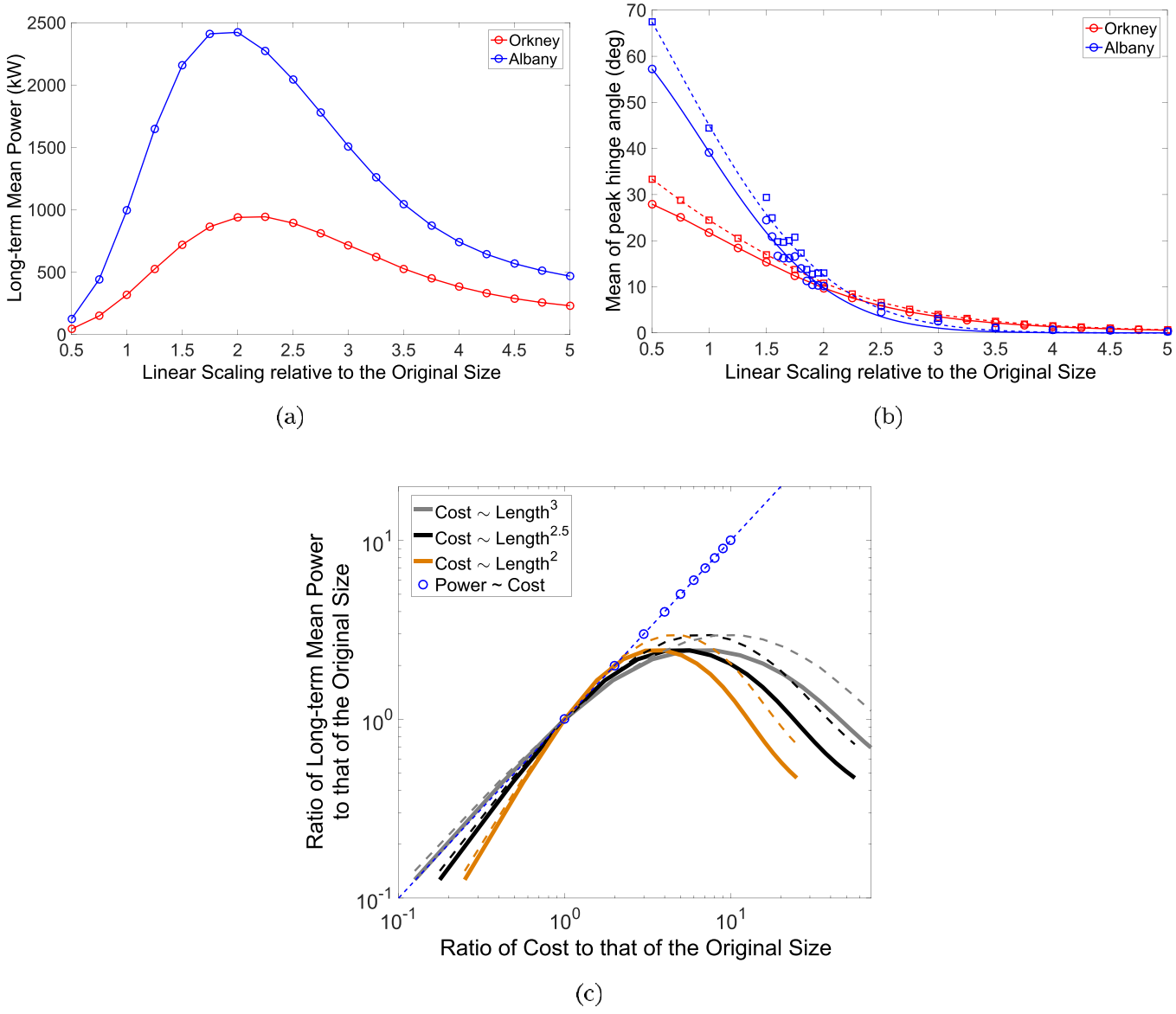

Fig. 14. Variation of the linear scaling of the original machine with (a) the long-term mean practical wave power output and (b) the long-term mean peak hinge angle. For (b), dashed line is for uni-directional sea-state, while solid line is for directional sea-state. (c) Variation of three lines (solid lines for Albany, dashed lines for Orkney) of normalised power output with cost ratio, assuming three variations of cost as a function of size. Also shown is the variation of normalised power output with the cost ratio of having more machines of the original size. Open circles denote integer numbers of multiple standard-sized machines.

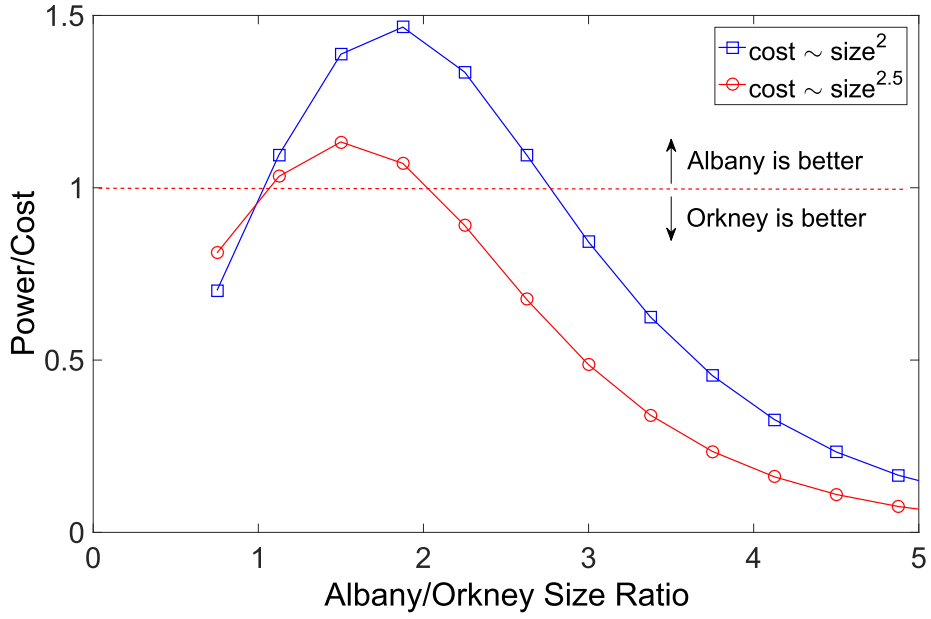

Fig. 15. Variation of the power to cost ratio with ratio of machine sized for Albany to Orkney for two different cost function assumptions.

7. Conclusions

The Australian coast is known to provide high wave energy densities (see Ref. [3]. To further possible development of wave power in Australia, we have presented analysis on both operability (power production) and survivability for the M4 machine in Albany and compared these to the EMEC test site on Orkney, north of Scotland. The Albany location is exposed to both storms and swells from the Southern Ocean. Orkney is exposed to some of the most severe winter storms in the eastern North Atlantic. Extreme waves at Albany are considerably less severe than anywhere in the exposed eastern North Atlantic and North Sea, particularly at 1 in 100 years and upwards. This has important implications for the survivability of any marine renewable energy device, in particular WECs. Looking at the mean energy wave period, Albany has a much longer period $T_e = 10.5$ sec compared to Orkney (EMEC) $T_e = 8.4$ sec, which shows that Albany is dominated by long-period swells from the Indian Ocean and Southern Oceans. And these swells are more stable over the year than the waves at Orkney.

With standard M4-machine sizing rules, we obtain a mean power production of 1 MW at Albany with an M4 machine length of 146 m compared to 319 kW for Orkney with a machine length of 94 m. Therefore, more wave energy per machine is available at Albany than Orkney. However, there are much larger predicted machine motions in severe storm conditions in Albany compared to Orkney, therefore threatening frequent component self-collision, at least using a linear model for the machine motion which would be reduced by nonlinear effects including dunking in practice. This can be greatly reduced by increasing the Albany machine size by $\times$ 1.5, and the survival rate becomes similar to that of Orkney, while at the same time increasing the average power output to 2.3 MW for Albany with machine length of 234 m. Comparing power to cost ratio between Albany and Orkney, with an Albany machine now $234/94 = 2.5\times$ larger than Orkney, we obtain the following:

- With cost $\sim$ size^2, power/cost $\sim$ 1.16$\times$ better for Albany vs. Orkney
- With cost $\sim$ size$^{2.5}$, power/cost $\sim$ 1.36$\times$ better for Orkney vs. Albany

Overall, since the cost is perhaps more likely to be somewhere between these two forms, there is not much difference in the performance of the optimised M4 machines at each of the two locations of Albany and Orkney. The higher power output efficiency and less pronounced seasonal effects (therefore more consistent power all year round) make Albany a slightly better location, in particular since the variability of the practical wave power at Orkney is strongly influenced by the variability of the waves in the winter in response to the combined effects of the North Atlantic Oscillation (NAO) and the higher geophysical atmospheric modes [19]. We also note that continuing improvement in the designs of M4-type machines could yield substantially more power per machine at lower cost/power [25].

We conclude with a comment about the Albany wind farm. There are 18 wind turbines in the Albany wind farm which is located on the top of the cliff above the wave energy site (see Fig. 3). The maximum capacity is 35.4 MW, which translates to 80% of the electricity requirements for the town of Albany. With a peak capacity of the optimum M4 machine at Albany of 7 MW (3$\times$ the mean power), 5 M4 machines would produce the same peak power output. More detailed economic analysis would be required to assess whether wave power at Albany would be a cost-effective replacement for the onshore wind farm.

Acknowledgements

We thank Jeff Hansen of UWA for providing the Australian wave buoy data. The real-time data is available from: https://www.transport.wa.gov.au/imarine/albany-tide-and-wave.asp.

Appendix

In addition to using the Weibull form shown in Equation (1), the exceedances are also fitted with the following variant form of Weibull distribution which is written as:

$$P = 1 - \exp\left[- \left(\frac{H_{mp} - H_c}{\alpha} \right)^{\beta} \right] \tag{7}$$

Fig. 16 plots the long-term extrapolation using the variant form of Weibull fit for Albany using fits to the whole year (12 months) and winter data (6 months only). There is little difference in the quality of the fits or the extrapolated values (here the extreme 1 in 1000 year H_{mp} is ~ 10% higher), so we conclude that our results are at least plausible.

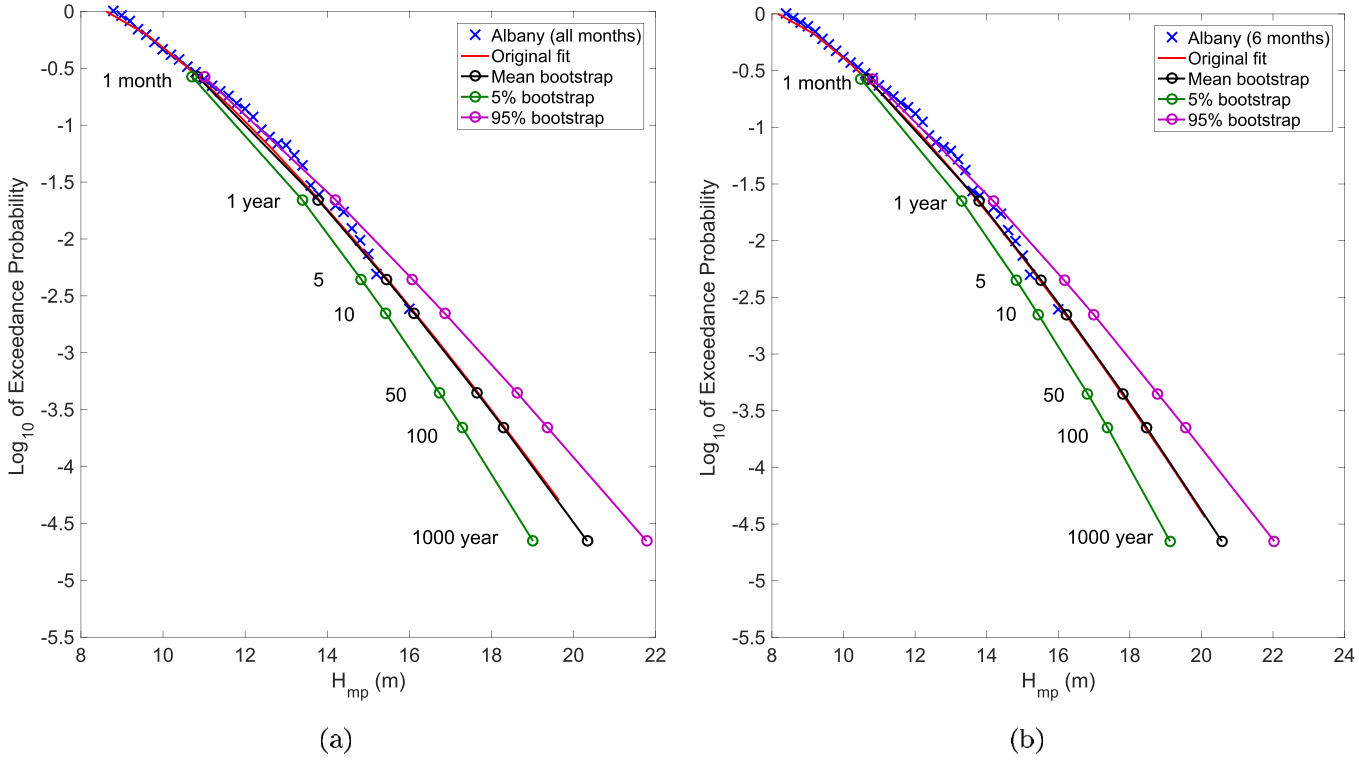

Fig. 16. Long-term extrapolation using the variant form of Weibull fit for Albany with threshold $N \sim 400$ largest storms and with (a) 12 ($\alpha = 0.9$ and $\beta = 1.3$) and (b) 6 months ($\alpha = 1.07$ and $\beta = 1.3$). The circles from bottom up correspond to H_{mp} with a return period of one in 1000 years, 100 years, 50 years, 10 years, 5 years, 1 year and 1 month, respectively.

References

[1] S. Ambühl, M. Sterndorff, J.D. Sørensen, Extrapolation of extreme response for different mooring line systems of floating wave energy converters, Int. J. Marine Energy 7 (2014) 1–19.

[2] A. Babarit, F. Wendt, Y.-H. Yu, J. Weber, Investigation on the energy absorption performance of a fixed-bottom pressure-differential wave energy converter, Appl. Ocean Res. 65 (2017) 90–101.

[3] S. Behrens, J.A. Hayward, S.C. Woodman, M.A. Hemer, M. Ayre, Wave energy for Australia's national electricity market, Renew. Energy 81 (2015) 685–693.

[4] W. Chen, I. Dolguntseva, A. Savin, Y. Zhang, W. Li, O. Svensson, M. Leijon, Numerical modelling of a point-absorbing wave energy converter in irregular and extreme waves, Appl. Ocean Res. 63 (2017) 90–105.

[5] R. Coe, Y.-H. Yu, J. van Rij, A survey of WEC reliability, survival and design practices, Energies 11 (1) (2017) 4.

[6] R. Eatock Taylor, P.H. Taylor, P.K. Stansby, A coupled hydrodynamic–structural model of the M4 wave energy converter, J. Fluids Struct. 63 (2016) 77–96.

[7] K.C. Ewans, Observations of the directional spectrum of fetch-limited waves, J. Phys. Oceanogr. 28 (3) (1998) 495–512.

[8] P. Jonathan, P.H. Taylor, On irregular, nonlinear waves in a spread sea, J. Offshore Mech. Arct. Eng. 119 (1997) 37.

[9] G. Lindgren, Some properties of a normal process near a local maximum, Ann. Math. Stat. (1970) 1870–1883.

[10] E.B. Mackay, A.S. Bahaj, P.G. Challenor, Uncertainty in wave energy resource assessment. Part 2: variability and predictability, Renew. Energy 35 (8) (2010) 1809–1819.

[11] M.J. Muliawan, Z. Gao, T. Moan, Application of the contour line method for estimating extreme responses in the mooring lines of a two-body floating wave energy converter, J. Offshore Mech. Arct. Eng. 135 (3) (2013a), 031301.

[12] M.J. Muliawan, M. Karimirad, Z. Gao, T. Moan, Extreme responses of a combined spar-type floating wind turbine and floating wave energy converter (STC) system with survival modes, Ocean Eng. 65 (2013b) 71–82.

[13] S. Parmeggiani, J.P. Kofoed, E. Friis-Madsen, Extreme loads on the mooring lines and survivability mode for the Wave Dragon wave energy converter, in: World Renewable Energy Congress 2011, 2011.

[14] E. Ransley, D. Greaves, A. Raby, D. Simmonds, M. Hann, Survivability of wave energy converters using CFD, Renew. Energy 109 (2017a) 235–247.

[15] E. Ransley, D. Greaves, A. Raby, D. Simmonds, M.M. Jakobsen, M. Kramer, RANS-VOF modelling of the Wavestar point absorber, Renew. Energy 109 (2017b) 49–65.

[16] M. Reistad, Ø. Breivik, H. Haakenstad, O.J. Aarnes, B.R. Furevik, J.-R. Bidlot, A high-resolution hindcast of wind and waves for the north sea, the Norwegian sea, and the Barents sea, J. Geophys. Res.: Oceans 116 (C5) (2011) 1978–2012.

[17] H. Santo, P.H. Taylor, E. Carpintero Moreno, P.K. Stansby, R. Eatock Taylor, L. Sun, J. Zang, Extreme motion and response statistics for survival of the three-float wave energy converter M4 in intermediate water depth, J. Fluid Mech. 813 (2017) 175–204.

[18] H. Santo, P.H. Taylor, R. Eatock Taylor, Y.S. Choo, Average properties of the largest waves in Hurricane Camille, J. Offshore Mech. Arct. Eng. 135 (2013), 011602.

[19] H. Santo, P.H. Taylor, R. Eatock Taylor, P.K. Stansby, Decadal variability of wave power production in the North-East Atlantic and North Sea for the M4 machine, Renew. Energy 91 (2016a) 442–450.

[20] H. Santo, P.H. Taylor, R. Gibson, Decadal variability of extreme wave height representing storm severity in the northeast Atlantic & North Sea since the foundation of the Royal Society, Proc. Math. Phys. Eng. Sci. 472 (2193) (2016b) 20160376.

[21] H. Santo, P.H. Taylor, T. Woollings, S. Poulson, Decadal wave power variability in the north-east Atlantic and North sea, Geophys. Res. Lett. 42 (12) (2015) 4956–4963.

[22] P. Schmitt, B. Elsaesser, On the use of OpenFOAM to model oscillating wave surge converters, Ocean Eng. 108 (2015) 98–104.

[23] W. Sheng, H. Li, J. Murphy, An improved method for energy and resource assessment of waves in finite water depths, Energies 10 (8) (2017) 1188.

[24] P.K. Stansby, E. Carpintero Moreno, T. Stallard, Capture width of the three-float multi-mode multi-resonance broadband wave energy line absorber M4

from laboratory studies with irregular waves of different spectral shape and directional spread, J. Ocean. Eng. Marine Energy (2015a) 1–12.
[25] P.K. Stansby, E. Carpintero Moreno, T. Stallard, Large capacity multi-float configurations for the wave energy converter M4 using a time-domain linear diffraction model, Appl. Ocean Res. 68 (2017) 53–64.
[26] P.K. Stansby, E. Carpintero Moreno, T. Stallard, A. Maggi, Three-float broad-band resonant line absorber with surge for wave energy conversion, Renew. Energy 78 (2015b) 132–140.
[27] P.H. Taylor, B.A. Williams, Wave statistics for intermediate depth water NewWaves and symmetry, J. Offshore Mech. Arct. Eng. 126 (2004) 54.
[28] P. Tromans, L. Vanderschuren, Response based design method in the North Sea: application of a new method, in: Offshore Technology Conference, OTC 7683, Houston, 1995.
[29] P.S. Tromans, A.R. Anaturk, P. Hagemeijer, A new model for the kinematics of large ocean waves, in: Proceedings of the International Society of Offshore and Polar Engineering Conference, ISOPE-91, 1991.
[30] Y.-H. Yu, Y. Li, Reynolds-Averaged Navier–Stokes simulation of the heave performance of a two-body floating-point absorber wave energy system, Comput. Fluid 73 (2013) 104–114.